

Geophysical Research Letters

RESEARCH LETTER

10.1029/2019GL086724

Key Points:

- We present subglacial topography models beneath Ekström, Atka, Jelbart, Fimbul, and Vigrid ice shelves
- Water cavities beneath ice shelves of wDML are secluded due to moraine formations at LGM and subsequent shallow water entry points
- Ice shelves are currently protected by sills but are highly sensitive to future warming ocean temperatures and changing thermocline depth

Supporting Information:

- Supporting Information S1

Correspondence to:

H. Eisermann,
heiserma@awi.de

Citation:

Eisermann, H., Eagles, G., Ruppel, A., Smith, E. C., & Jokat, W. (2020). Bathymetry beneath ice shelves of western Dronning Maud Land, East Antarctica, and implications on ice shelf stability. *Geophysical Research Letters*, 47, e2019GL086724. <https://doi.org/10.1029/2019GL086724>

Received 18 DEC 2019

Accepted 27 APR 2020

Accepted article online 3 MAY 2020

Bathymetry Beneath Ice Shelves of Western Dronning Maud Land, East Antarctica, and Implications on Ice Shelf Stability

Hannes Eisermann¹ , Graeme Eagles¹ , Antonia Ruppel² , Emma Clare Smith¹ , and Wilfried Jokat^{1,3} 

¹Alfred-Wegener-Institute, Bremerhaven, Germany, ²Federal Institute for Geosciences and Natural Resources, Hannover, Germany, ³Faculty of Geosciences, University of Bremen, Bremen, Germany

Abstract Antarctica's ice shelves play a key role in stabilizing the ice streams that feed them. Since basal melting largely depends on ice-ocean interactions, it is vital to attain consistent bathymetry models to estimate water and heat exchange beneath ice shelves. We have constructed bathymetry models beneath the ice shelves of western Dronning Maud Land by inverting airborne gravity data and incorporating seismic, multibeam, and radar depth references. Our models reveal deep glacial troughs beneath the ice shelves and terminal moraines close to the continental shelf breaks, which currently limit the entry of Warm Deep Water from the Southern Ocean. The ice shelves buttress a catchment that comprises an ice volume equivalent to nearly 1 m of eustatic sea level rise, partly susceptible to ocean forcing. Changes in water temperature and thermocline depth may accelerate marine-based ice sheet drainage and constitute an underestimated contribution to future global sea level rise.

Plain Language Summary The grounded ice sheets of Antarctica are stabilized by floating ice shelves. Any loss in ice shelf mass is matched by an increase in ice sheet drainage, which contributes to rising sea level. The ice shelves of western Dronning Maud Land are currently in balance with an inland ice volume that has the potential to raise global sea level by nearly 1 m. Ice shelves lose most of their mass from their bases when warm water intrudes from the surrounding ocean. The extent to which this occurs depends on the depth and shape of the seafloor beneath the ice shelves. We have modeled water depths beneath the ice shelves of Dronning Maud Land using airborne gravity data and depth measurements from seismic, multibeam, and radar data. Our bathymetric models show deep troughs beneath the ice shelves and shallow sills close to the continental shelf. These sills currently limit water mass exchange with Warm Deep Water from the Southern Ocean and so protect the ice shelves from significant melting at their bases. A changing climate with increasing ocean temperatures or a shallowing of warm water masses may increase ice shelf melting and lead to an increased sea level contribution.

1. Introduction

Floating ice shelves in Antarctica play a key role in buttressing its grounded continental ice sheets. Freezing and/or melting at ice shelf bases influences the overall mass balance of the ice sheets that feed them. An increase in mass loss of an ice shelf is followed by increased drainage of its ice sheet (Dupont & Alley, 2005; Gudmundsson et al., 2019). The most important process by which Antarctica's ice shelves lose mass is basal melting by interactions with warm seawater (Depoorter et al., 2013; Oerter et al., 1992; Rignot et al., 2013), whose circulation beneath the shelves largely depends on subglacial bathymetry (An et al., 2019; Jenkins et al., 2010; Tinto et al., 2019). According to Goldberg et al. (2019), accurate bathymetry is the leading requirement for correctly estimating basal melt rates in circulation models. Consistent and accurate bathymetric models therefore benefit estimations of ice shelf and ice sheet stability. However, most compilations of subglacial topography incorporate low-resolution interpolated sub-ice shelf bathymetries (Arndt et al., 2013; Fretwell et al., 2013; Morlighem et al., 2019).

The cavities beneath the ice shelves of western Dronning Maud Land (wDML) have been only sparsely and incompletely sounded by seismic reflection data on the Fimbul and Ekström ice shelves (Nøst, 2004; Smith et al., 2020). Bathymetry beneath the neighboring Atka, Jelbart, and Vigrid ice shelves is simply unknown. Covering 63,000 km² (Figure 1), they represent 10% of East Antarctica's total ice shelf by area and experience

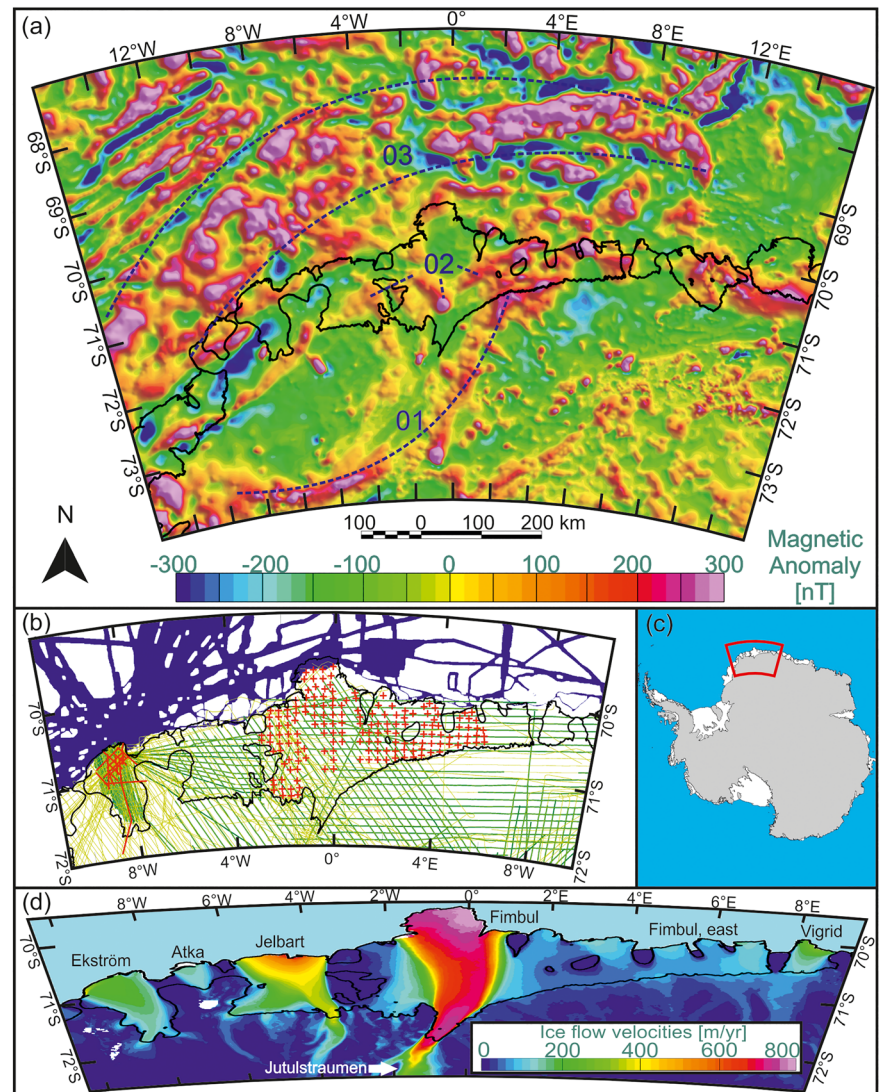


Figure 1. Overview of survey region in wDML with (a) magnetic anomaly data (Golynsky et al., 2018; Mieth & Jokat, 2014) showing the proposed boundary of the Archaean Grunehogna Craton (Unit 01), Jurassic mafic intrusions (Unit 02), and seaward dipping Jurassic basalt flows (Unit 03) (Jokat et al., 2003, 2004; Riedel et al., 2013). (b) Map of data used for this study with gravity (green) and ice thickness radar data (yellow), bathymetric references from prevalent seismic reflection data (red), and shipborne swath bathymetry data (blue). (c) Extent of survey region. Grounded ice, ice shelves, and ocean are illustrated in gray, white, and blue, respectively. (d) Ice flow velocities showing main drainage areas of wDML after Mouginit et al. (2017b).

mass loss predominately from iceberg calving and basal melting in almost equal parts (Rignot et al., 2013). The ice shelves' catchment area is mainly drained through the Jutulstraumen Glacier (Figure 1; Mouginit et al., 2017b; Rignot et al., 2013). The area currently contains 341,000 Gt of ice above sea level, a sea level equivalent (SLE) of about 0.95 m (Supporting Information S1). Around 18% (17 cm SLE) of this is grounded below current sea level, making it susceptible to ocean forcing. Inland, where prograde slopes impair ocean intrusion to the remaining catchment, mass loss is expected to be dominated by atmospheric forcing (DeConto & Pollard, 2016).

The ice shelves of wDML are in contact with seawater at temperatures close to the surface freezing point. This classifies them as cold-cavity ice shelves (Rignot et al., 2013). Increasing water temperatures in cavities are generally related to warming ocean temperatures (Gille, 2008; Schmidtko et al., 2014), redirected currents, or increased upwelling of Warm Deep Water (WDW; Carmack & Foster, 1975; Hattermann, 2018; Schröder & Fahrbach, 1999). WDW is carried by the Weddel Gyre traversing a narrow continental shelf at

wDML (Schröder & Fahrbach, 1999), permitting strong interaction between the coastal current and water cavities and implying high sensitivity to rising ocean temperatures (Nicolaus & Grosfeld, 2004). Increasing temperature could lead to a rapid increase in basal melt rates and negatively influence ice shelf mass balance (Hellmer et al., 2012). Langley, von Deschanden, et al. (2014) observed a network of inverted channels at the base of the Fimbul Ice Shelf using ground-based radar data, hinting at small-scale active melting. In addition, Zhou et al. (2014) have shown that heated Antarctic Surface Water (ASW) finds its way beneath the Fimbul Ice Shelf, whereas the entry of WDW is currently minimal and strongly dependent on bathymetric features (Hattermann et al., 2014).

We address the lack of consistent and reliable bathymetric estimates beneath the ice shelves of wDML by inversion of airborne gravity data for bathymetry. Our models reveal deep troughs beneath the ice shelves and allow us to identify sites of possible present or future inflow of WDW into the cavities.

1.1. Geologic Framework

A clear understanding of underlying geology is vital for modeling bathymetry from gravity because of the effects of variable rock densities on gravitational accelerations (Brisbourne et al., 2014). The geology of wDML is largely interpreted by extrapolation from sparse outcrops along magnetic anomalies (Jacobs et al., 1998; Jacobs et al., 2017, Figure 1a). This reveals strong geologic affinities to South Africa, its conjugate in Gondwana (Jokat et al., 2003). The Archean Grunehogna Craton represents a fragment of the Kalahari-Kaapvaal-Craton (Jacobs & Thomas; 2004, Riedel et al., 2013, Figure 1a, Unit 01). Semicircular lineaments over the Jelbart and Fimbul ice shelves represent Jurassic olivine-gabbro intrusions into the eastern part of the craton (Ferraccioli et al., 2005; Golynsky & Aleshkova, 2000; Riedel et al., 2013, Figure 1a, Unit 02). The adjacent Mesoproterozoic Maud-Belt of deformed and metamorphosed continental rocks is equivalent to the African Namaqua-Natal Belt (Jacobs et al., 2015; Jacobs & Thomas, 2004; Mueller & Jokat, 2019).

Along the continental shelf, a belt of strongly positive magnetic anomalies (Figure 1a, Unit 03) is related to thick packages of intercalated basalts and sediments that dip toward the ocean, as interpreted in seismic reflection data (Kristoffersen et al., 2014). Beneath the Ekström Ice Shelf, these basalt packages form the so-called Explora Wedge (Hinz & Krause, 1982; Jokat et al., 2004; Kristoffersen & Haugland, 1986), which we describe in greater detail in section 3.1 using newly acquired high-resolution magnetic data.

2. Materials and Methods

Bathymetry models for the Ekström and Atka ice shelves are based on aerogeophysical data collected during the austral summer of 2015/2016 within the Geodynamic evolution of East Antarctica (GEA) project conducted by the Alfred Wegener Institute (AWI) and Federal Institute for Geosciences and Natural Resources (BGR). The Fimbul and Vigrid bathymetry models are based on data collected between 2001 and 2004 as part of AWI's VISA project (Riedel et al., 2012). Bathymetric models for Jelbart are based on a compilation of GEA and VISA data. Both projects collected coincident gravity, magnetic, and radio echo sounding (RES) data (Figure 1b). Seismic data are incorporated for Ekström (Smith et al., 2020) and Fimbul ice shelves (Nøst, 2004).

Gravity data of differing quality were delivered by a GT-2A gravimeter during the GEA campaign and a ZLS Ultrasys Lacoste & Romberg Air/Sea gravimeter during VISA campaigns (Figure S2.1; Riedel et al., 2012). Confidence in the bathymetric models also depends on the availability of reliable ancillary information on subsurface geological density variations. Our estimates of combined uncertainties in the model bathymetries are ± 175 m (Ekström and Atka), ± 225 m (Jelbart), and ± 210 m (Fimbul and Vigrid), consistent with previous empirically derived root mean square misfits between inversion-derived and seismic depths for other Antarctic ice shelves (Brisbourne et al., 2014; Greenbaum et al., 2015).

Gravity data are inverted for bathymetry using the module "GM-SYS 3D" within Geosoft Oasis montaj, which implements a 3D forward-modeling approach based on Parker (1972). Reference and control points from seismic data over the ice shelves, swath bathymetry along the calving fronts, and grounded ice thickness from RES data are used where available to design preprocessing filters to suppress nonbathymetric signals. These specific filters are applied to enhance the resemblance between gravity and sparsely known existing bathymetric data (Figures 2 and 3) as a step toward minimizing residuals prior to inversions. Free-air anomaly (FAA) data over the Ekström and Atka ice shelves (Figure 2a) were preprocessed using

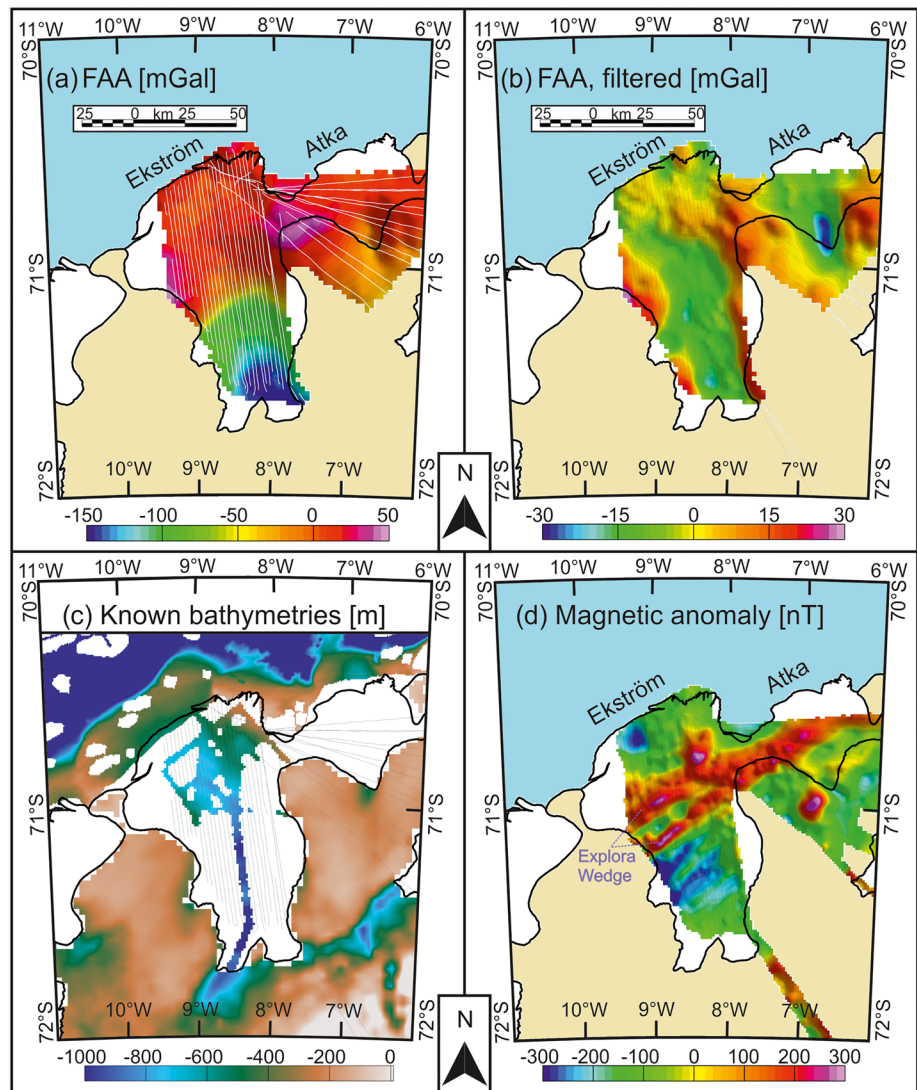


Figure 2. Known bathymetries and free-air anomaly (FAA) data above Ekström and Atka ice shelves with a flight line spacing of 2 to 5 km (gravimetric and magnetic flight lines in white). Grounded ice, open water, and ice shelves are marked in beige, blue, and white, respectively. The unfiltered FAA data (a) are filtered with a high-pass and directional filter (b) to achieve a starting resemblance to constrained bathymetries (c) from swath bathymetry, seismic reflection data (Smith et al., 2020), and ice thickness radar data in grounded areas. New high-resolution magnetic anomaly data are depicted in panel (d) with linear magnetic highs interpreted as seaward dipping basalt flows associated with the Explora Wedge.

a 70-km high-pass filter, oriented at 45° using a cosine function to suppress features trending parallel to the main crustal and geological structures of the continental shelf, as revealed in the magnetic anomaly data (Figure 2d). FAA data from the Jelbart Ice Shelf were isotropically band-pass filtered over 6–100 km (Figures 3a and 3b), and those across the Fimbul and Vigrid ice shelves were band-pass filtered over 6–150 km (Figures 3c and 3d) to suppress aircraft noise and long wavelength signals related to crustal thickness variations and sedimentary basins at the extended continental margin (Figure 3; Jokat et al., 2003, 2004).

RES ice thicknesses from the GEA campaign are derived after correction for firn (Blindow, 1994) and subtraction from the Reference Elevation Model of Antarctica (REMA; Howat et al., 2019) to determine the base ice position. Ice thicknesses from VISA campaigns are incorporated from Riedel et al. (2012).

Along the coastline and calving fronts of wDML, swath bathymetry data acquired during various surveys conducted by RV *Polarstern* are implemented to evaluate the progression of possible troughs

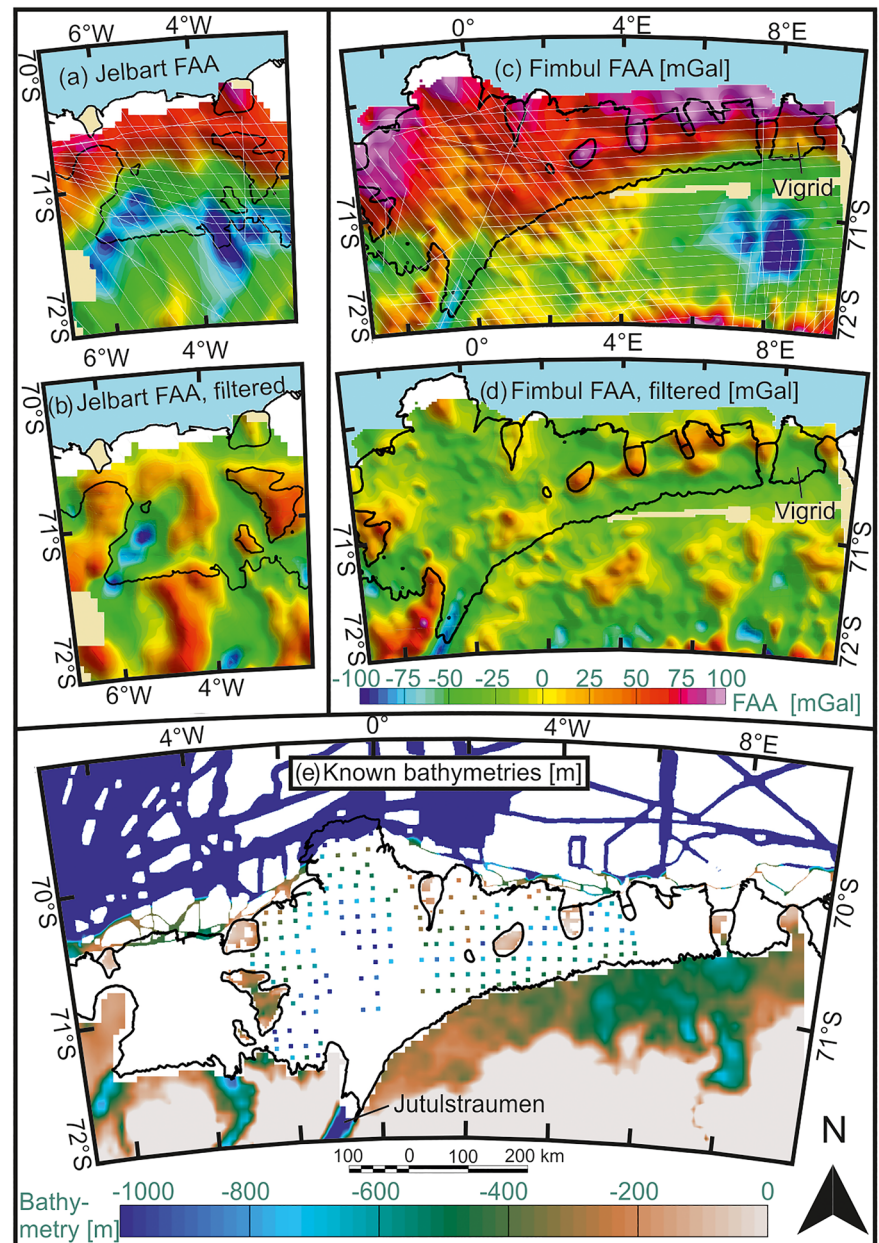


Figure 3. Known bathymetries and free-air anomaly (FAA) data across Jelbart, Fimbul, and Vigrud ice shelves. The unfiltered FAA data for Jelbart (a) and Fimbul/Vigrud (c) with crossing flight lines (5- to 10-km spacing) are band-pass filtered in panels (b) and (d) to achieve a starting resemblance to bathymetries (e) constrained from swath bathymetry, seismic reflection point data (Nøst, 2004; 5×5 -km squares), and ice thickness radar data in grounded areas. Positive, long-wavelength anomalies close to the continental shelf in the north in panels (a) and (c), possibly representing crustal thinning, were removed by described filtering techniques in panels (b) and (d). Legend in panel (d) is valid for panels (a) through (d).

toward the continental shelf. Grounding lines and coastal boundaries are taken from Mouginot et al. (2017a).

Airborne magnetic data across wDML were acquired during the GEA campaign using a Scintrex Cs-3 cesium magnetometer, including at 2-km line spacing above Ekström (Figure 2d). We used these data to interpret shallow subsurface geological variations at wavelengths passed by prefiltering that must be accounted for in bathymetric modeling (Figure 1). For further details on materials and methods, see Supporting Information S2.

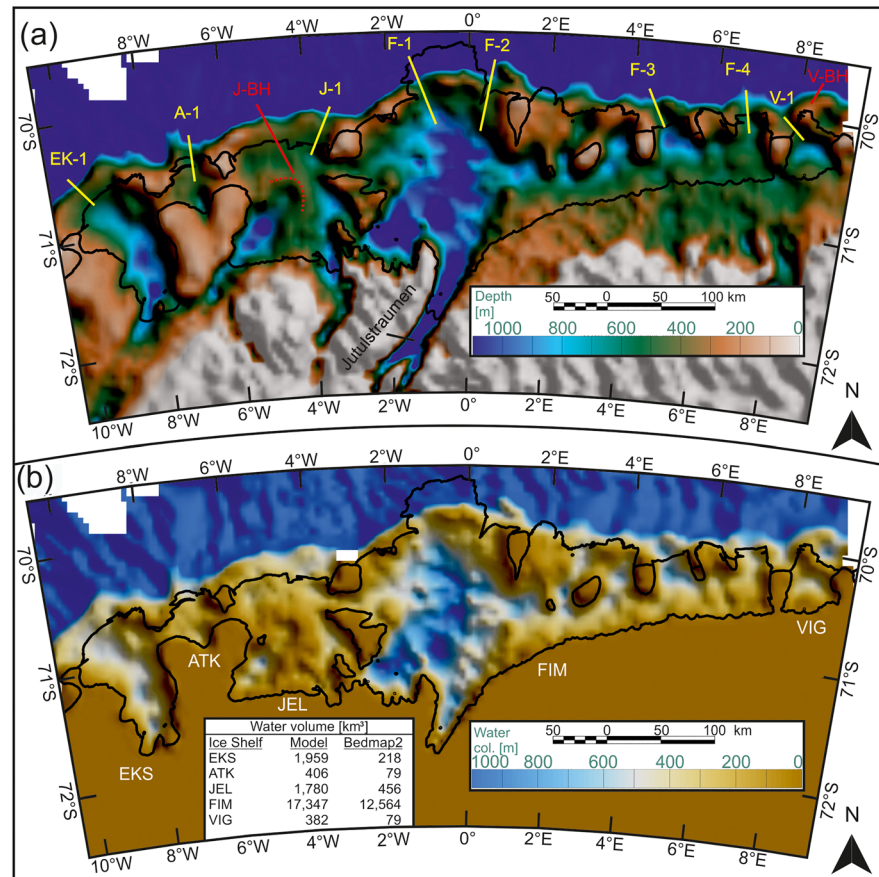


Figure 4. Subglacial bathymetry and water column thickness beneath ice shelves of wDML. (a) Bathymetry, relative to WGS84, exhibits secluded shelf ice cavities with distinct gateways marked for each ice shelf (yellow, EK-1, A-1, J-1, F-1 to F-4, V-1). Bathymetric highs and former possible pinning points can be inferred in the center of Jelbart (J-BH) and the north of Vigrid Ice Shelf (V-BH). The water column thickness (b) is inferred from newly generated bathymetries and ice draft (Riedel et al., 2012). Table in panel (b) compares water volume in km^3 of the new, updated model presented in this paper with water volume from Bedmap2 (Fretwell et al., 2013). Grounding line and ice shelf extents are incorporated after Mouginito et al. (2017a).

3. Results

3.1. Geologic Constraints From Magnetic Data Interpretation

Changes in magnetic field strength are far less sensitive to bathymetric than to geological variations, meaning well-founded magnetic interpretations can be employed to reduce uncertainty in the gravity models. SW–NE-trending positive magnetic anomalies oriented perpendicular to the ice shelf flow are identified in the aeromagnetic data set across the Ekström Ice Shelf (Figure 2d). A linear high reaching 250 nT in the eastern part of Ekström bifurcates westwards into 300-nT-high branches. These anomalies are confidently related to the shallow subcrop of the Explora Wedge (Kristoffersen et al., 2014). Ferraccioli et al. (2005) and Riedel et al. (2013) interpret a triangular magnetic high across the Jelbart Ice Shelf and coincident circular gravity and magnetic anomaly highs over the southern part of the Fimbul Ice Shelf close to the outlet of the Jutulstraumen (Figure 1a, Unit 02) as Jurassic mafic intrusions. These intrusions are reflected in the density maps estimated in the 3D modeling process (Supporting Information S2) showing a distinct correlation to magnetic anomalies.

3.2. Bathymetric Models Beneath Ice Shelves of wDML

Figure 4 shows models of bathymetry beneath the ice shelves, together with water column thicknesses estimated by subtraction of the ice draft calculated from RES data. Our first-order observation in wDML is that the ice shelves overlie a seabed (mostly <1 km deep) that deepens between shallow sills close to the

present-day calving fronts and the landward grounding line. In greater detail, troughs cross the shelves, and the sills are interrupted by a series of distinct narrow gateways (Figure 4a). Depth maxima, especially beneath the Ekström and Fimbul ice shelves, correlate with thick water columns and are separated by small bathymetry highs. This may result in several possible water circulation regimes (Figure 4).

Modeled bathymetry beneath the Ekström Ice Shelf is characterized by a trough parallel to the direction of main ice flow (Figures 1d and 4a). It has two distinct maxima with water depths of about 1,130 m in the south and 1,030 m in the center separated by a bathymetric high of 860 m. The water column (Figure 4b) is thickest over the trough, with maxima slightly exceeding 600 m in the south and center, interrupted by the bathymetric high. Swath bathymetry along the calving front shows a 390-m-deep gateway to the cavity (EK-1, Figure 4a) within a sill following the course of the calving front.

The neighboring Atka Ice Shelf has a similar shape, with a NNW-trending trough in its center exhibiting two depth maxima, at 780 m modeled close to the grounding line and 620 m, observed in bathymetry data, north of the calving front. Gateways in the sill reach an observed depth of 500 m beyond the calving front and a modeled depth of 450 m beneath the ice shelf (A-1, Figure 4).

The Jelbart Ice Shelf is underlain by two bathymetric troughs, separated by a broad bathymetric high over which the water column thins to 50 m. The western trough reaches maximum depths of 1,200 and 1,050 m in the south separated by a minor bathymetric high. The trough terminates against a rampart-like bathymetric high (J-BH, Figure 4a). The eastern trough coincides with the present-day surface ice flow maximum (Figure 1d). Its maximum depth is about 1,000 m close to the grounding line and 900 m in its center. It progresses north toward the continental shelf edge where it crosses a bathymetric sill via a 430-m-deep gateway, observed with swath bathymetry, into the Weddell Sea (J-1, Figure 4a).

The seabed beneath the Fimbul Ice Shelf is characterized by a central trough in line with the Jutulstraumen glacier outlet (Figure 1d). Three depth maxima of 1,300, 1,250, and 1,150 m, from south to north, are set between 1,000-m-deep bathymetric highs. The main gateway, F-1 (Figure 4a), is located at the central trough's projection to the shelf-edge sill with its deepest point modeled at 550 m. Three additional gateways are modeled, one 70 km further east (F-2) at a depth of 450 m and two others in the east at 530 m (F-3) and 600 m (F-4) depths. The deepest point overall beneath Fimbul lies in the SW at 1,370 m.

Further east, bathymetry beneath the Vigrid Ice Shelf is generally quite shallow. Maximum water depths of 600 m are modeled beneath the central part of the ice shelf. A single 450 m deep gateway is modeled on its western side (V-1, Figure 4). The northern part of the ice shelf overlies a shallow area with a cavity height of just 40 m beneath relatively fast-flowing ice (Figure 1d).

4. Discussion

Smith et al. (2020) report large differences between seismically derived depths beneath the Ekström Ice Shelf and those derived by interpolation in Bedmap2 (Fretwell et al., 2013), which has been the baseline data set for the majority of modeling studies in the area. Our models show similar differences, reaching up to several hundreds of meters, for all ice shelves of wDML. Based on these differences, Bedmap2 underestimates the volume of wDML water cavities by 63% compared to our bathymetric models. Excluding the area of Nøst's (2004) seismic measurements, which were incorporated in Bedmap2, Bedmap2 underestimates cavity volume by 444% (table in Figure 4b), because it interpolates between the sparse reference points.

Seabed variations beneath the ice shelves of wDML are all of similar shapes, including deep troughs separated by small bathymetric highs, suggesting shared or related origins and former glacier extents. Smith et al. (2020) interpret periodic retreat of the grounding line position based on the presence of multiple bathymetric highs interspersed between deep points along the trough beneath Ekström. Our bathymetric model displays similar features and shows the bathymetric highs to continue laterally across the seafloor, supporting this interpretation. We also observe similar segmentation of troughs crossing the neighboring ice shelves.

These troughs vanish in shallow water close to the calving fronts. The repetition of this pattern throughout wDML suggests a link to former glacial extents, most likely via the formation of end moraines by ice sheets that advanced to the continental shelf edges during the Last Glacial Maximum (LGM, at 23–19 kyr BP; Grobe & Mackensen, 1992; Hillenbrand et al., 2014). Subglacial sediments deposited at shelf edges might be

displaced downslope or be remobilized by currents to form contourites, as observed in seismic data close to the ice shelves of Dronning Maud Land by Huang and Jokat (2016).

The modern-day calving fronts of these ice shelves overlie shallow sills cut by gateways with depth maxima at 550 to 600 m, which limit the possible entry of WDW (Schröder & Fahrbach, 1999) into the cavities due to similar average thermocline depths of about 600 m in water depths of 1,000 m (Hattermann, 2018). Hattermann et al. (2014) have shown that only small amounts of modified WDW creeps into the Fimbul cavity. The sills thus currently protect the ice shelf base from basal melting from considerable WDW ingress. Seasonal variability in basal melting beneath Fimbul (Langley, Kohler, et al., 2014) is probably linked to the inflow of solar-heated ASW (Zhou et al., 2014). A similar setting for neighboring ice shelves leads to the assumption that present-day basal melting processes are mainly driven by ASW throughout wDML. Our new results show long continuous cavities at depths greater than 1,000 m leading landwards from the sills at average depths of 400 m. If enhanced surface ocean warming or a shallower thermocline in the future leads more significant quantities of warm water to breach the sills, these deep troughs will guide fast access to the grounding line with little to stop basal melting from eroding wDML's ice shelves. Since our bathymetric models are limited by their depth uncertainties and a horizontal resolution of about 5 km, it is necessary to further investigate these decisive bathymetric features close to the calving fronts in the future.

Buttressing by grounding at pinning points plays an important role in stabilizing ice shelves by braking ice flow (Dupont & Alley, 2005). We suggest that a broad bathymetric high with a water column of 50 m in the center of the Jelbart Ice Shelf (J-BH, Figure 4a) acted as a pinning point in the past. This semicircular bathymetric high suggests its formation as a moraine, caused by former glacial extents at the western trough and/or less erosion in the center of the ice shelf due to main ice streams being situated west and east. From this we infer a depositional character for J-BH, whose depth may be underestimated owing to unaccounted-for lower density. Loss of buttressing might explain a high ice mass loss of 41 Gt for the drainage area of the Jelbart Ice Shelf from 1979 until 2017, compared to stable mass balances in neighboring drainage areas (Rignot et al., 2019). A similar paleo-pinning point (V-BH, Figure 4a) is interpretable from the short (40 m) water column beneath the northern Vigrid Ice Shelf. Buttressing loss from these points might have led to enhanced thinning and accelerated drainage (Dupont & Alley, 2005); ice flow velocities over the Vigrid Ice Shelf are currently faster than the neighboring eastern Fimbul Ice Shelf (Figure 1d). However, ice velocities have not increased in the time span from 1994 to 2012 (Gudmundsson et al., 2019).

5. Summary

We have constructed new bathymetric models for seafloor beneath the Ekström, Atka, Jelbart, Fimbul, and Vigrid ice shelves using gravity inversions constrained by seismic, multibeam, and radar data and geological variability interpreted from magnetic anomalies. Our bathymetric models show that current topographic compilations used, for example, in ice sheet/ocean modeling heavily underestimate the vulnerable ice shelf cavities of wDML by up to 798% for the Ekström Ice Shelf and by 63% in total.

The newly mapped seabed underlies about 10% of East Antarctica's ice shelf inventory by area (Rignot et al., 2013). It is of direct significance for understanding and modeling the current and future stability of the wDML ice sheet, which contains water equivalent to about 0.95 m of eustatic sea level rise and is susceptible to ocean and atmospheric forcing.

The models show deep seawater cavities under all of the ice shelves, providing increasing evidence that this is a trend in DML. These cavities are partially secluded from the open ocean by sills perched near or at the continental shelf edge. The sills currently protect the ice shelves from basal melting by WDW ingress. At present, the ice shelves probably experience basal melting mainly by warm surface waters. However, shallowing thermocline depths with an increased entry of WDW into the cavities pose a significant risk to these ice shelves in the future.

Data Availability Statement

Bathymetric models and raw gravity data can be accessed at pangaea.de (10.1594/PANGAEA.913742).

Acknowledgments

GEA is jointly funded by the Alfred Wegener Institute (AWI) and the Federal Institute for Geosciences and Natural Resources (BGR). Seismic data beneath Fimbul and Ekström were supplied by the Norwegian Polar Institute and the Alfred Wegener Institute (Glaciology), respectively. ECS was funded through the AWI-BGR Sub-EIS-Obs project and grant EI672/10-1 "Cost-S2S" by the Deutsche Forschungsgemeinschaft (DFG) in the framework of the priority programme "Antarctic Research with comparative investigations in Arctic ice areas. The authors would like to thank Emerson E&P Software, Emerson Automation Solutions, for providing licenses for the seismic software Paradigm in the scope of the Emerson Academic Program. We are grateful to two anonymous reviewers, whose comments greatly enhanced the manuscript. We thank the science and technician crew of airborne campaigns as well as the crews of RV *Polarstern* and the AWI bathymetry group for acquiring and processing bathymetry data.

References

An, L., Rignot, E., Chauche, N., Holland, D. M., Holland, D., Jakobsson, M., et al. (2019). Bathymetry of Southeast Greenland from Oceans Melting Greenland (OMG) data. *Geophysical Research Letters*, *46*(20), 11,197–11,205. <https://doi.org/10.1029/2019gl083953>

Arndt, J. E., Schenke, H. W., Jakobsson, M., Nitsche, F. O., Buys, G., Goleby, B., et al. (2013). The International Bathymetric Chart of the Southern Ocean (IBCSO) version 1.0—A new bathymetric compilation covering circum-Antarctic waters. *Geophysical Research Letters*, *40*(12), 3111–3117. <https://doi.org/10.1002/grl.50413>

Blindow, N. (1994). The central part of the Filchner-Ronne Ice Shelf, Antarctica: Internal structures revealed by 40MHz monopulse RES. *Annals of Glaciology*, *20*, 365–371. <https://doi.org/10.1017/S0260305500016700>

Brisbourne, A., Smith, A., King, E., Nicholls, K., Holland, P., & Makinson, K. (2014). Seabed topography beneath Larsen C Ice Shelf from seismic soundings. *The Cryosphere*, *8*(1), 1–13. <https://doi.org/10.5194/tc-8-1-2014>

Carmack, E. C., & Foster, T. D. (1975). On the flow of water out of the Weddell Sea. *Paper presented at the Deep Sea Research and Oceanographic Abstracts*, *22*(11), 711–724. [https://doi.org/10.1016/0011-7471\(75\)90077-7](https://doi.org/10.1016/0011-7471(75)90077-7)

DeConto, R. M., & Pollard, D. (2016). Contribution of Antarctica to past and future sea-level rise. *Nature*, *531*(7596), 591–597. <https://doi.org/10.1038/nature17145>

Depoorter, M. A., Bamber, J. L., Griggs, J. A., Lenaerts, J. T., Ligtenberg, S. R., van den Broeke, M. R., & Moholdt, G. (2013). Calving fluxes and basal melt rates of Antarctic ice shelves. *Nature*, *502*(7469), 89–92. <https://doi.org/10.1038/nature12567>

Dupont, T., & Alley, R. B. (2005). Assessment of the importance of ice-shelf buttressing to ice-sheet flow. *Geophysical Research Letters*, *32*, L04503. <https://doi.org/10.1029/2004GL020224>

Ferraccioli, F., Jones, P., Curtis, M., & Leat, P. (2005). Subglacial imprints of early Gondwana break-up as identified from high resolution aerogeophysical data over western Dronning Maud Land, East Antarctica. *Terra Nova*, *17*(6), 573–579. <https://doi.org/10.1111/j.1365-3121.2005.00651.x>

Fretwell, P., Pritchard, H. D., Vaughan, D. G., Bamber, J. L., Barrand, N. E., Bell, R., et al. (2013). Bedmap2: Improved ice bed, surface and thickness datasets for Antarctica. *The Cryosphere*, *7*(1), 375–393. <https://doi.org/10.5194/tc-7-375-2013>

Gille, S. T. (2008). Decadal-scale temperature trends in the Southern Hemisphere ocean. *Journal of Climate*, *21*(18), 4749–4765. <https://doi.org/10.1175/2008jcli2131.1>

Goldberg, D., Gourmelen, N., Kimura, S., Millan, R., & Snow, K. (2019). How accurately should we model ice shelf melt rates? *Geophysical Research Letters*, *46*(1), 189–199. <https://doi.org/10.1029/2018GL080383>

Golynsky, A. V., & Aleshkova, N. D. (2000). Regional magnetic anomalies of the Weddell Sea region and their geological significance. *Polarforschung*, *67*(3), 101–117.

Golynsky, A. V., Ferraccioli, F., Hong, J. K., Golynsky, D. A., von Frese, R. R. B., Young, D. A., et al. (2018). New magnetic anomaly map of the Antarctic. *Geophysical Research Letters*, *45*(13), 6437–6449. <https://doi.org/10.1029/2018gl078153>

Greenbaum, J. S., Blankenship, D. D., Young, D. A., Richter, T. G., Roberts, J. L., Aitken, A. R. A., et al. (2015). Ocean access to a cavity beneath Totten Glacier in East Antarctica. *Nature Geoscience*, *8*(4), 294–298. <https://doi.org/10.1038/Ngeo2388>

Grobe, H., & Mackensen, A. (1992). Late Quaternary climatic cycles as recorded in sediments from the Antarctic continental margin. *The Antarctic paleoenvironment: A perspective on Global Change; Antarctic Research Series*, *56*, 349–376.

Gudmundsson, G. H., Paolo, F. S., Adusumilli, S., & Fricker, H. A. (2019). Instantaneous Antarctic ice-sheet mass loss driven by thinning ice shelves. *Geophysical Research Letters*, *46*, 13,903–13,909. <https://doi.org/10.1029/2019GL085027>

Hattermann, T. (2018). Antarctic thermocline dynamics along a narrow shelf with easterly winds. *Journal of Physical Oceanography*, *48*(10), 2419–2443. <https://doi.org/10.1175/Jpo-D-18-0064.1>

Hattermann, T., Smedsrud, L. H., Nøst, O. A., Lilly, J. M., & Galton-Fenzi, B. K. (2014). Eddy-resolving simulations of the Fimbul Ice Shelf cavity circulation: Basal melting and exchange with open ocean. *Ocean Modelling*, *82*, 28–44. <https://doi.org/10.1016/j.ocemod.2014.07.004>

Hellmer, H. H., Kauker, F., Timmermann, R., Determann, J., & Rae, J. (2012). Twenty-first-century warming of a large Antarctic ice-shelf cavity by a redirected coastal current. *Nature*, *485*(7397), 225–228. <https://doi.org/10.1038/nature11064>

Hillenbrand, C. D., Bentley, M. J., Stollendorf, T. D., Hein, A. S., Kuhn, G., Graham, A. G. C., et al. (2014). Reconstruction of changes in the Weddell Sea sector of the Antarctic Ice Sheet since the Last Glacial Maximum. *Quaternary Science Reviews*, *100*, 111–136. <https://doi.org/10.1016/j.quascirev.2013.07.020>

Hinz, K., & Krause, W. (1982). The continental margin of Queen Maud Land, Antarctica: Seismic sequences, structural elements and geological development. *Geologisches Jahrbuch. Reihe E, Geophysik*, *23*, 17–41.

Howat, I. M., Porter, C., Smith, B. E., Noh, M. J., & Morin, P. (2019). The Reference Elevation Model of Antarctica. *The Cryosphere*, *13*(2), 665–674. <https://doi.org/10.5194/tc-13-665-2019>

Huang, X. X., & Jokat, W. (2016). Sedimentation and potential venting on the rifted continental margin of Dronning Maud Land. *Marine Geophysical Research*, *37*(4), 313–324. <https://doi.org/10.1007/s11001-016-9296-x>

Jacobs, J., Elburg, M., Läufer, A., Kleinhanns, I. C., Henjes-Kunst, F., Estrada, S., et al. (2015). Two distinct Late Mesoproterozoic/Early Neoproterozoic basement provinces in central/eastern Dronning Maud Land, East Antarctica: The missing link, 15–21 degrees E. *Precambrian Research*, *265*, 249–272. <https://doi.org/10.1016/j.precamres.2015.05.003>

Jacobs, J., Fanning, C. M., Henjes-Kunst, F., Olesch, M., & Paech, H. J. (1998). Continuation of the Mozambique Belt into East Antarctica: Grenville-age metamorphism and polyphase Pan-African high-grade events in central Dronning Maud Land. *Journal of Geology*, *106*(4), 385–406. <https://doi.org/10.1086/516031>

Jacobs, J., Opås, B., Elburg, M. A., Läufer, A., Estrada, S., Ksienzyk, A. K., et al. (2017). Cryptic sub-ice geology revealed by a U-Pb zircon study of glacial till in Dronning Maud Land, East Antarctica. *Precambrian Research*, *294*, 1–14. <https://doi.org/10.1016/j.precamres.2017.03.012>

Jacobs, J., & Thomas, R. J. (2004). Himalayan-type indenter-escape tectonics model for the southern part of the late Neoproterozoic-early Paleozoic East African-Antarctic orogen. *Geology*, *32*(8), 721–724. <https://doi.org/10.1130/G20516.1>

Jenkins, A., Dutrieux, P., Jacobs, S. S., McPhail, S. D., Perrett, J. R., Webb, A. T., & White, D. (2010). Observations beneath Pine Island Glacier in West Antarctica and implications for its retreat. *Nature Geoscience*, *3*(7), 468–472. <https://doi.org/10.1038/Ngeo890>

Jokat, W., Boebel, T., Koenig, M., & Meyer, U. (2003). Timing and geometry of early Gondwana breakup. *Journal of Geophysical Research*, *108*(B9), 2428. <https://doi.org/10.1029/2002JB001802>

Jokat, W., Ritzmann, O., Reichert, C., & Hinz, K. (2004). Deep crustal structure of the continental margin off the Explora Escarpment and in the Lazarev Sea, East Antarctica. *Marine Geophysical Researches*, *25*(3–4), 283–304. <https://doi.org/10.1007/s11001-005-1337-9>

- Kristoffersen, Y., & Haugland, K. (1986). Geophysical evidence for the East Antarctic plate boundary in the Weddell Sea. *Nature*, 322(6079), 538–541. <https://doi.org/10.1038/322538a0>
- Kristoffersen, Y., Hofstede, C., Diez, A., Blenkner, R., Lambrecht, A., Mayer, C., & Eisen, O. (2014). Reassembling Gondwana: A new high quality constraint from vibroseis exploration of the sub-ice shelf geology of the East Antarctic continental margin. *Journal of Geophysical Research: Solid Earth*, 119, 9171–9182. <https://doi.org/10.1002/2014JB011479>
- Langley, K., Kohler, J., Sinisalo, A., Øyan, M. J., Hamran, S. E., Hattermann, T., et al. (2014). Low melt rates with seasonal variability at the base of Fimbul ice shelf, East Antarctica, revealed by in situ interferometric radar measurements. *Geophysical Research Letters*, 41(22), 8138–8146. <https://doi.org/10.1002/2014gl061782>
- Langley, K., von Deschanden, A., Kohler, J., Sinisalo, A., Matsuoka, K., Hattermann, T., et al. (2014). Complex network of channels beneath an Antarctic ice shelf. *Geophysical Research Letters*, 41(4), 1209–1215. <https://doi.org/10.1002/2013gl058947>
- Mieth, M., & Jokat, W. (2014). Fresh view on the geological fabric of eastern Dronning Maud Land. *East Antarctica, Gondwana Research*, 25(1), 358–367. <https://doi.org/10.1016/j.gr.2013.04.003>
- Morlighem, M., Rignot, E., Binder, T., Blankenship, D., Drews, R., Eagles, G., et al. (2019). Deep glacial troughs and stabilizing ridges unveiled beneath the margins of the Antarctic Ice Sheet. *Nature Geoscience*, 13(2), 132–137. <https://doi.org/10.1038/s41561-019-0510-8>
- Mouginot, J., Scheuchl B., & Rignot E. (2017a). MEASURES Antarctic Boundaries for IPY 2007-2009 from Satellite Radar, version 2. Boulder, Colorado USA. NASA National Snow and Ice Data Center Distributed Active Archive Center. <https://doi.org/10.5067/AXE4121732AD>. [10/2019].
- Mouginot, J., Scheuchl B., & Rignot E. (2017b). MEASURES Annual Antarctic Ice Velocity Maps 2005-2017, version 1. [2016-2017]. Boulder, Colorado USA. NASA National Snow and Ice Data Center Distributed Active Archive Center. <https://doi.org/10.5067/9T4EPQXTJYW9>. [10/2019]
- Mueller, C. O., & Jokat, W. (2019). The initial Gondwana break-up: A synthesis based on new potential field data of the Africa-Antarctica Corridor. *Tectonophysics*, 750, 301–328. <https://doi.org/10.1016/j.tecto.2018.11.008>
- Nicolaus, M., & Grosfeld, K. (2004). Ice-ocean interactions underneath the Antarctic ice shelf Ekströmsisen. *Polarforschung*, 72(1), 17–29.
- Nøst, O. A. (2004). Measurements of ice thickness and seabed topography under the Fimbul ice shelf, Dronning Maud Land, Antarctica. *Journal of Geophysical Research*, 109, C10010. <https://doi.org/10.1029/2004JC002277>
- Oerter, H., Kipfstuhl, J., Determann, J., Miller, H., Wagenbach, D., Minikin, A., & Graf, W. (1992). Evidence for basal marine ice in the Filchner-Ronne ice shelf. *Nature*, 358(6385), 399–401. <https://doi.org/10.1038/358399a0>
- Parker, R. (1972). The rapid calculation of potential anomalies. *Geophysical Journal International*, 31(4), 447–455.
- Riedel, S., Jacobs, J., & Jokat, W. (2013). Interpretation of new regional aeromagnetic data over Dronning Maud Land (East Antarctica). *Tectonophysics*, 585, 161–171. <https://doi.org/10.1016/j.tecto.2012.10.011>
- Riedel, S., Jokat, W., & Steinhage, D. (2012). Mapping tectonic provinces with airborne gravity and radar data in Dronning Maud Land, East Antarctica. *Geophysical Journal International*, 189(1), 414–427. <https://doi.org/10.1111/j.1365-246X.2012.05363.x>
- Rignot, E., Jacobs, S., Mouginot, J., & Scheuchl, B. (2013). Ice-shelf melting around Antarctica. *Science*, 341(6143), 266–270. <https://doi.org/10.1126/science.1235798>
- Rignot, E., Mouginot, J., Scheuchl, B., van den Broeke, M., van Wessem, M. J., & Morlighem, M. (2019). Four decades of Antarctic Ice Sheet mass balance from 1979-2017. *Proceedings of the National Academy of Sciences of the United States of America*, 116(4), 1095–1103. <https://doi.org/10.1073/pnas.1812883116>
- Schmidtko, S., Heywood, K. J., Thompson, A. F., & Aoki, S. (2014). Multidecadal warming of Antarctic waters. *Science*, 346(6214), 1227–1231. <https://doi.org/10.1126/science.1256117>
- Schröder, M., & Fahrback, E. (1999). On the structure and the transport of the eastern Weddell Gyre. *Deep Sea Research Part II: Topical Studies in Oceanography*, 46(1–2), 501–527. [https://doi.org/10.1016/S0967-0645\(98\)00112-X](https://doi.org/10.1016/S0967-0645(98)00112-X)
- Smith, E. C., Hattermann, T., Kuhn, G., Gaedicke, C., Berger, S., Drews, R., et al. (2020). Detailed Seismic Bathymetry Beneath Ekström Ice Shelf, Antarctica: Implications for Glacial History and Ice-Ocean Interaction. *Geophysical Research Letters*, 47(10), e2019GL086187. <https://doi.org/10.1029/2019gl086187>
- Tinto, K. J., Padman, L., Siddoway, C. S., Springer, S. R., Fricker, H. A., Das, I., et al. (2019). Ross Ice Shelf response to climate driven by the tectonic imprint on seafloor bathymetry. *Nature Geoscience*, 12(6), 441–449. <https://doi.org/10.1038/s41561-019-0370-2>
- Zhou, Q., Hattermann, T., Nøst, O., Biuw, M., Kovacs, K., & Lydersen, C. (2014). Wind-driven spreading of fresh surface water beneath ice shelves in the Eastern Weddell Sea. *Journal of Geophysical Research: Oceans*, 119, 3818–3833. <https://doi.org/10.1002/2013JC009556>